ClaRa+ Quality Management: On Validation of Implemented Physics

Detailed Description of the Validation Efforts at the ClaRa+ Development Team

Document version 2, Date: 16. July, 2019, linked to ClaRa+ release 1.2.1

Authors

Timm Hoppe, Dr. Friedrich Gottelt, Ales Vojacek
XRG Simulation GmbH
Harburger Schlossstr. 6-12
21079 Hamburg, Germany

Contact

www.powerplantsimulation.com | info@powerplantsimulation.com

Legal Notices

ClaRa+ is an enhancement of ClaRa which was funded by the German Ministry of Economic Affairs and Energy (grants 03ET2009 and 03ET7060)

Supported by:
Federal Ministry for Economic Affairs and Energy
on the basis of a decision by the German Bundestag

Content

Scope of This Document

To validate the ClaRa^{+} library models of different level of complexity are compared with intra-day measurement data or with data from literature. With each new version of the ClaRa^{+} these validation scenarios are used for regression testing of the library. For more details on the ClaRa^{+} quality management efforts see (ClaRa+ Development Team, 2018). From the total group of validation scenarios some representative examples are presented in this paper and the results are discussed in detail. These examples illustrate the scope of the library and give insight to the regression testing process.

The basic thermo-hydraulic tests are for validation of the most basic models, e.g. like pressure loss models. They are applied in component models. The validation of the basic models gives deep insight into correct implementation of physics.

The component tests aim at validating arrangements of basic models representing technical aggregates. A good example for such an aggregate is a heat exchanger model which makes use of basic fluid and solid volumes, heat transfer and pressure loss correlations. Component tests also illustrate the range of validity of a model.

System model validation has another purpose. Correct implementation of single components or even basic models can hardly be concluded from the validation results. However, it gives valuable information on the scope of the library. Most important is the regression testing of these real life applications.

Basic Thermo-Hydraulic Tests

Validation of Shell Heat Transfer

Two sets of literature data on heat transfer at the shell side of a shell-and-tube heat exchanger are used for validation of ClaRa+ shell and heat transfer models, namely VLE_HT.NusseltShell1ph_L2 for one-phase shell flows and VLE_HT.NusseltShell2ph_L2 for two-phase shell flows. The one-phase data is from (VDI-Wärmeatlas, Gh. Wärmeübertragung im Außenraum von Rohrbündelwärmeübertragern mit Umlenkblechen., 2002) and the two-phase data is from (Fujii, 1970).

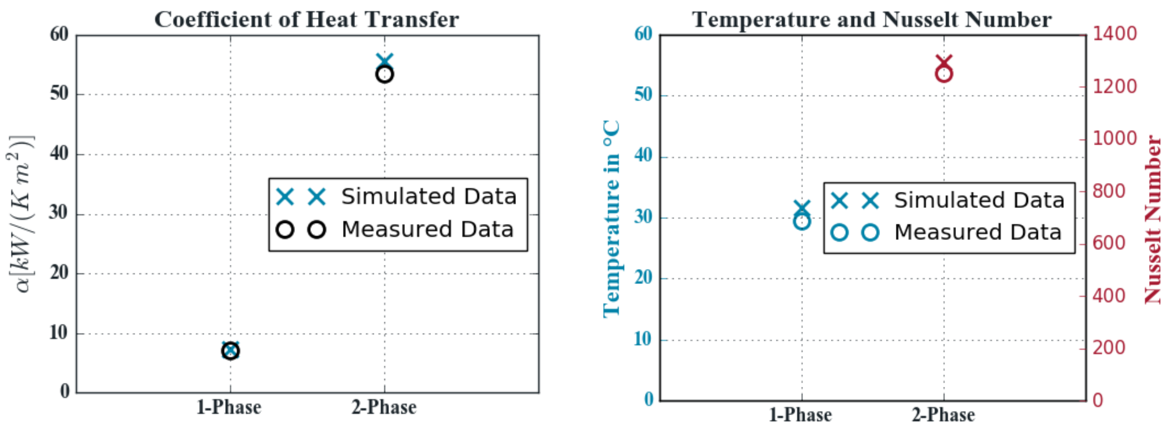

Figure 1: Heat transfer coefficient, temperature and Nusselt number of shell heat transfer validation

In Figure 1 the results obtained with the simulation models and the literature data are shown. The simulated data is in good accordance with the data from literature. It can be concluded that the heat transfer model, as well as the shell model and its interaction with the fluid properties are implemented correctly.

Validation of One-Phase Pipe Heat Transfer

The heat transfer of the pipe model is investigated for a broad range of Reynolds numbers and compared to data from (VDI-Wärmeatlas, Ga. Wärmeübertragung bei der Strömung durch Rohre., 2002).

Figure 2 shows the results of the comparison. The data from literature is met very well. The implementation of the pipe model, the heat transfer model and its interaction with the fluid properties are valid over a broad range of Reynolds numbers.

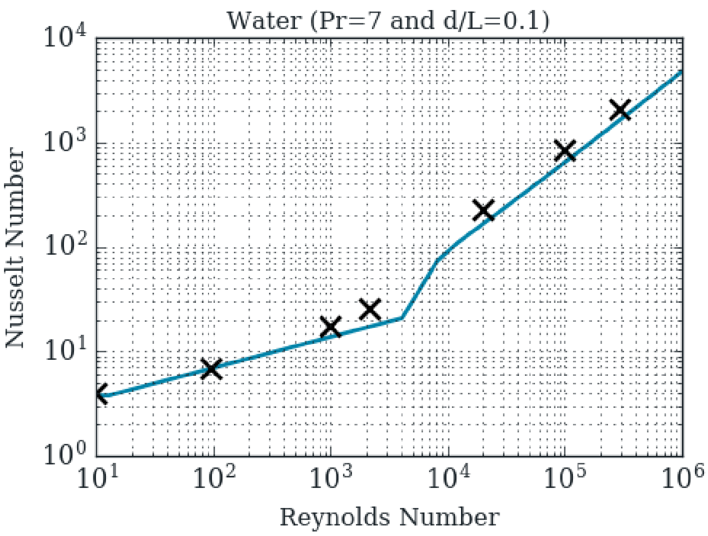

Figure 2: Heat transfer coefficient of one-phase pipe heat transfer validation

Validation of Two-Phase Pipe Pressure Loss

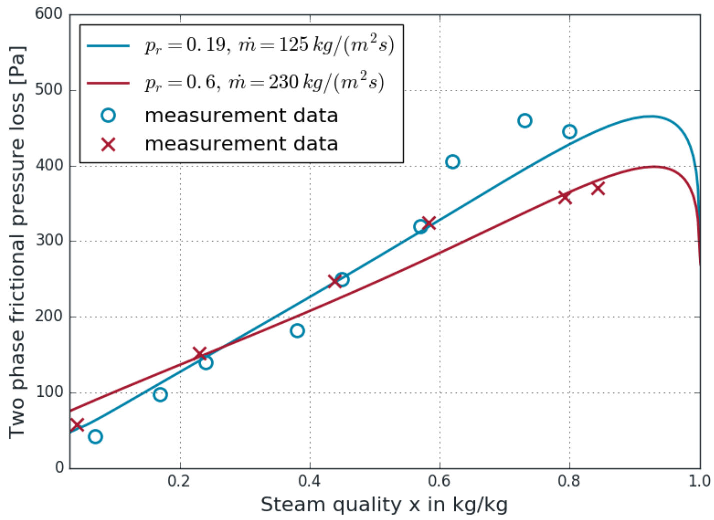

Figure 3: Two-phase pressure loss validation

The pressure loss of a two-phase medium in the ClaRa+ pipe model is investigated and compared to measurements. The measurements are taken from (Müller-Steinhagen, 1984). However, the data is not completely independent. It is part of the database from which the pressure loss correlation used in the ClaRa+ was derived, see (H. Müller-Steinhagen, 1986).

Figure 3 shows the results of the comparison for boiling nitrogen. The pressure loss is plotted over the steam quality indicating good accordance.

Validation of Bend Pressure Loss

The ClaRa+ model of a bend bases on the pressure loss model presented in (Idelchik, 2006). It is validated against measurements from (VDI-Wärmeatlas, La. Druckverlust in Leitungen mit Querschnittsänderungen., 2002).

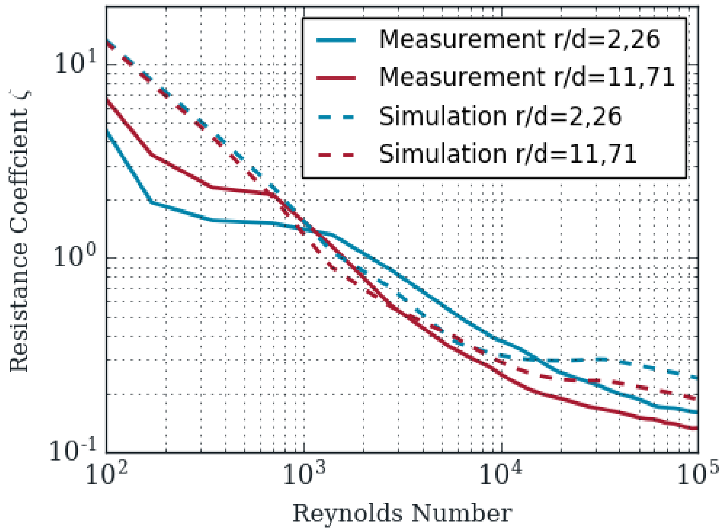

Figure 4: Validation of Bend Pressure Loss for 90° Bends

Figure 4 shows the resistance coefficient plotted against the Reynolds number for 90° bends of two different bend radius to inner diameter ratios. The simulated results fit very well for the technical relevant area, which are turbulent flows with a Reynolds number larger than at least 1000.

Validation of Relief Valve Outflow Function

The ClaRa$^+$ relief valve and its derivative model for an orifice base on the isentropic homogeneous equilibrium model (HEM), e.g. described in (Henry & Fauske, 1971). It assumes that the vapour and the liquid phase in the vena contracta are in mechanical and thermal equilibrium. The big advantage of the model is the validity for the whole range from liquid to two-phase and gaseous flows with mathematically continuous transitions. The mass flow through the vena contracta can be calculated from the stagnation conditions, i.e. the inlet conditions, without knowledge of the outlet conditions. At low stagnation steam qualities or at slightly subcooled stagnation conditions the present flow patterns have a large slip between the phases. In consequence, the assumption of mechanical equilibrium is not justified. In these cases, the HEM approach can lead to deviations of the calculated mass flows. The deviations usually underestimate the mass flux which is conservative for sizing of the valve. The relief valve model is compared with measurements from (Diener & Schmidt, 2004) who have measured the critical mass flux at different stagnation steam qualities and pressures.

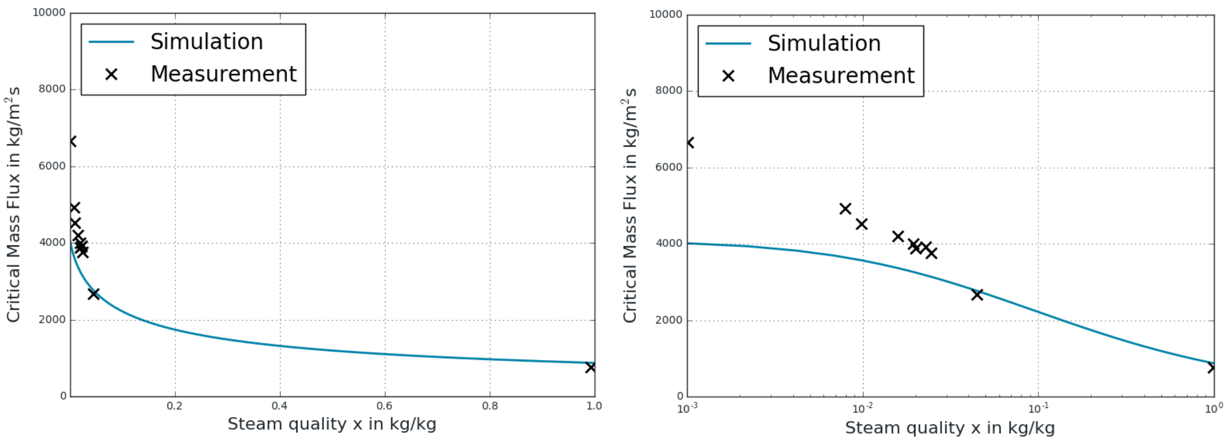

Figure 5: Validation of calculated critical mass flux of relief valve model with 0.68 MPa stagnation pressure on normal (left) and logarithmic scale (right)

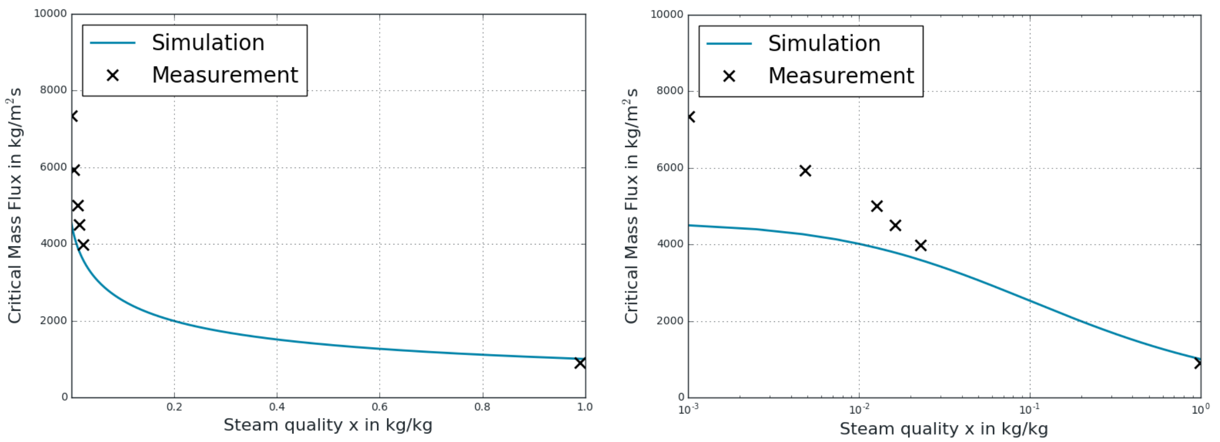

Figure 6: Validation of calculated critical mass flux of relief valve model with 0.8 MPa stagnation pressure on normal (left) and logarithmic scale (right)

Figure 5 and Figure 6 show critical mass flux at two different stagnation pressures plotted over the stagnation steam quality at logarithmic and normal scale. At steam qualities higher than 0.01 kg/kg the deviations are below 15%. At steam qualities larger than 0.05 kg/kg the simulation results are in perfect match with the measurements. Only at very low steam qualities larger deviations of up to 40 % can be observed. This finding is in accordance with the restrictions of the HEM model concerning the mechanical equilibrium of the phases.

Super Cannon Experiment

A model of the Super Cannon Blow Down experiment is built with ClaRa⁺ components. The experiment was designed to validate nuclear security codes, e.g. ATHLET or TRACE, and to examine their capability of modelling a loss of cooling accident (LOCA). This is an application clearly beyond the original scope of the system modelling tool ClaRa⁺. However, it provides valuable information on the scope of the basic thermo-hydraulic models of the ClaRa⁺ and it is therefore discussed here. The experiment is described in (Riegel, 1979), the measurement data is taken from (Saha, Jo, Neymotin, Rohatgi, & Slovik, 1981).The experiment setup is as follows: A horizontal pipe of 4.389 m with sealed faces is filled with hot water at 150 bar and 280 °C. At the beginning of the experiment one face of the pipe is opened by destroying a rupture disk. The water starts to flow out through the opening and the pressure decreases accordingly. With decreasing pressure evaporation and phase separation occurs. Pressure and void fraction are measured with respect to time and special distribution. Figure 7 right shows a schematic of the experiment taken from (Saha, Jo, Neymotin, Rohatgi, & Slovik, 1981) and on the left the system model in ClaRa⁺.

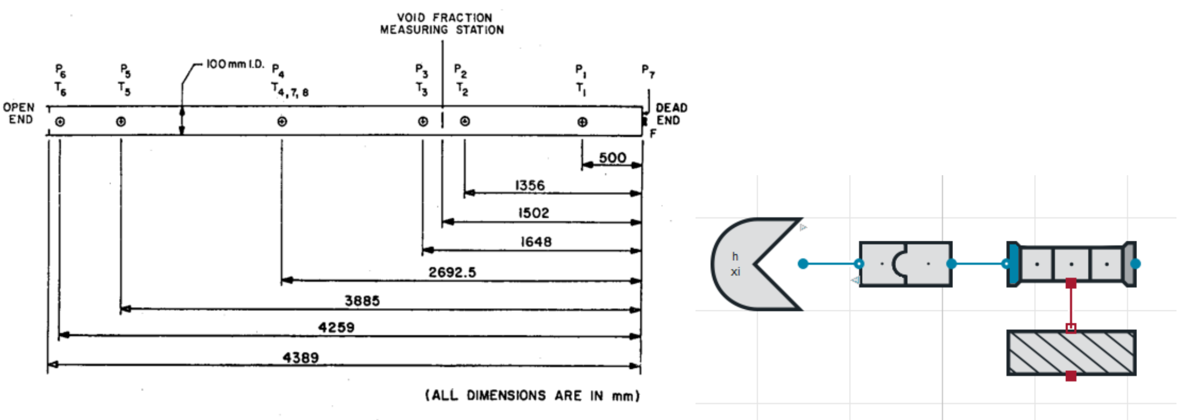

Figure 7: Schematic of the Super Cannon Test Section and its representation in ClaRa⁺

For modelling the pipe, the ClaRa⁺ advanced pipe is parametrised with the geometry from the experiment. The rupture disc is modelled by the ClaRa⁺ burst disk model with a two-phase outflow function and a constant discharge coefficient of 0.95.

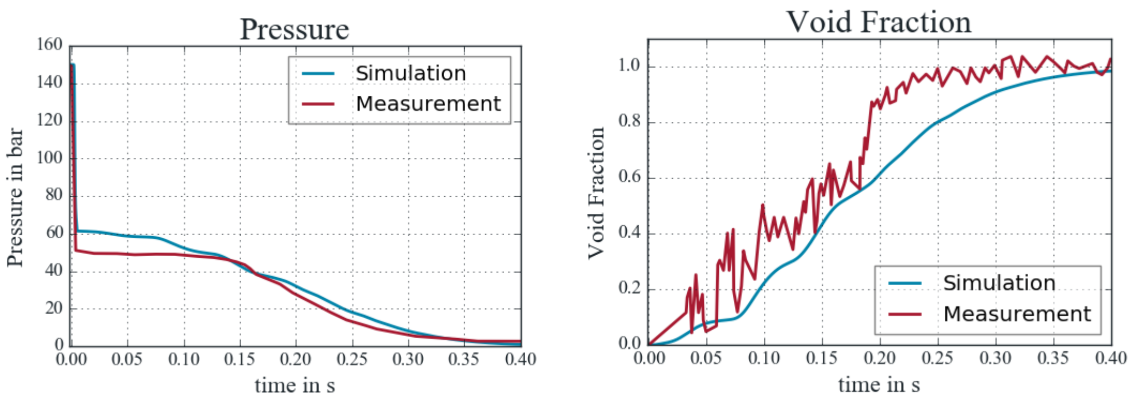

Figure 8: Pressure and void fraction at one third of total pipe length of Super Cannon Blowdown experiment

This value is within the limits for rupture discs given in (Friedel, 1998). A duration of 10 ms is assumed for the opening process of the rupture disk. The void fraction is calculated by a model published in (Zivi, 1964).

The comparison of the simulation results with the pressure measurements is shown in Figure 8 left. The measurements were taken at one third of the pipe length from the dead end. The pressure decay is met quite well by the model. However, in the first 100 ms no undershoot below the saturation pressure can be observed in the simulation. This is due to the lack of a flashing delay model in the ClaRa⁺ pipe, which would account for the delayed beginning of evaporation. To keep ClaRa⁺ models suitable for system simulation and as simple and robust as possible an implementation of such a model was not considered so far.

The outgoing mass flow rate was not measured in the experiment. The good prediction of the pressure decay in the pipe indicates that the simulated mass flow is in good accordance with the experiment. As can be seen in Figure 8 right the void fraction is also well predicted by the simulation.

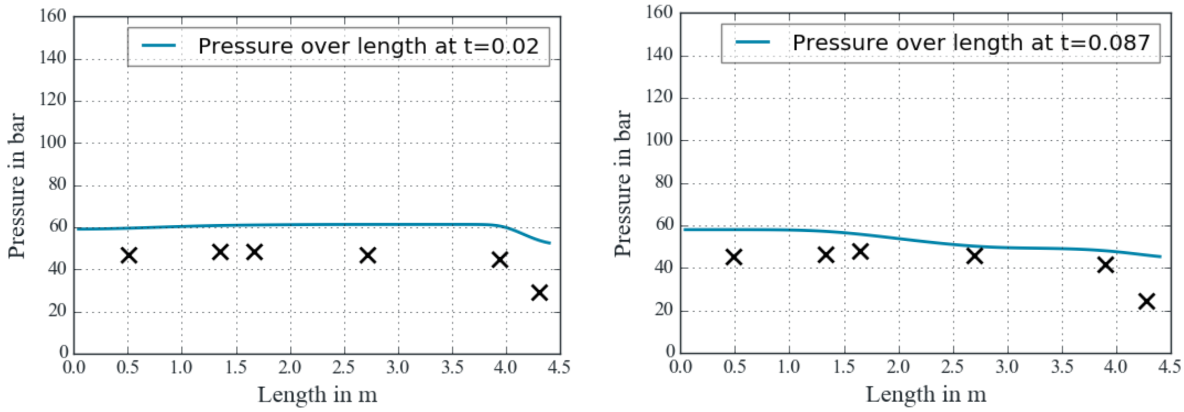

Figure 9: Pressure over pipe length at different times of Super Cannon Blowdown experiment

The pressure was measured in the experiment at different positions of the pipe, the comparison of the simulation results with the measurement at 20 ms and 87 ms is plotted in Figure 9. The delayed evaporation in the experimental results can also be observed in these plots. The pressure in the simulation stays at saturation pressure, while the measured pressure falls below saturation point. It leads to a relative error of approximately 15%, see Figure 9 left. At 87 ms, i.e. Figure 9 right, the fluid in the experiment begins to evaporate in the second half of the pipe. The measured pressure is in good accordance with the simulation. As can be seen in Figure 8 left the given errors can be considered as worst case estimations since the accuracy of the model increases significantly after the first 100 ms when evaporation starts.

At the pipe's outlet a deviation of nearly 50 % between measured and simulated pressure must be observed. This issue has to be discussed more in detail. Choked flow conditions and large pressure gradients are present at the outlet. As the ClaRa^{+} pipe model is not capable of representing choked flow conditions, mainly due to numerical reasons, the burst disk component with an appropriate pressure loss model is used to model the pressure relief to atmosphere. That means that the expansion to atmospheric pressure is not modelled as a locally distributed effect but concentrated in the burst disk component. Therefore, no intermediate pressures during the expansion process can be accessed in the simulation results. The simulated pressures in the pipe are pressures before expansion of the fluid. From a system scope of view (and as long as a spatially distributed information on the expansion process is not needed) this approach is completely sufficient.

The overall emptying process on a larger time scale, i.e. more than 100 ms, is represented very well by the model. Furthermore, the experiment gives insight into the correct implementation of basic thermo-hydraulic effects. The hold of the pressure decay at saturation pressure and the beginning evaporation can be observed in the simulation. Thus, energy from the thermal masses of the pipe, e.g. pipe wall, is used for evaporation. A requirement for prediction of this effect is the correct implementation of energy conservation, heat transfer and its interaction with fluid properties. From correct prediction of the emptying process, one can conclude that basic mass conservation is also fulfilled in ClaRa$^+$ pipe model.

Further reading on sudden depressurization of vessels:

- OECD Standard Problem No.6 – Depressurization of a vessel: (HOLZER, KANZLEITER, & STEINHOFF, 1977)
- Physical phenomena during depressurization: (Mayinger, 1987)

Component Tests

Steam Turbine

The ClaRa+ steam turbine model, SteamTurbineVLE_L1, is validated with measurements from a 600 MW hard coal plant. The high pressure part of the turbine to first tapping is modelled according to manufacturer's data. The boundary conditions of the scenario are presented in Figure 10.

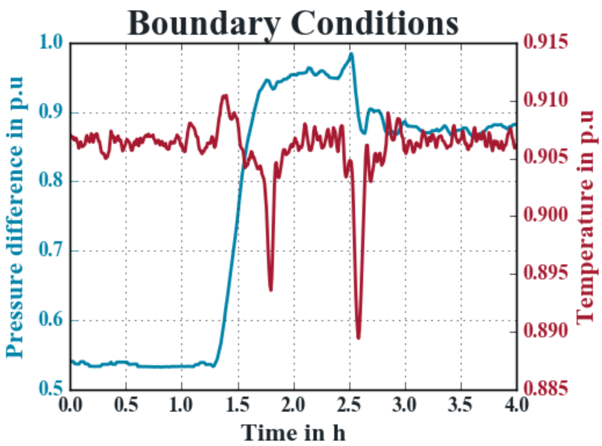

Figure 10: Boundary conditions of steam turbine validation

During the scenario a pressure gradient of 80 bar is induced to the turbines inlet at 1.5 hours, while small variations in pressure prevail the whole time. Two drops in the outlet temperature at 1.75 hours and 2.5 hours are observed in the scenario. As additional boundary condition, which is not shown in the figure, the backpressure of the turbine outlet is taken from the measurement. Figure 11 shows the comparison of measurement and simulation result.

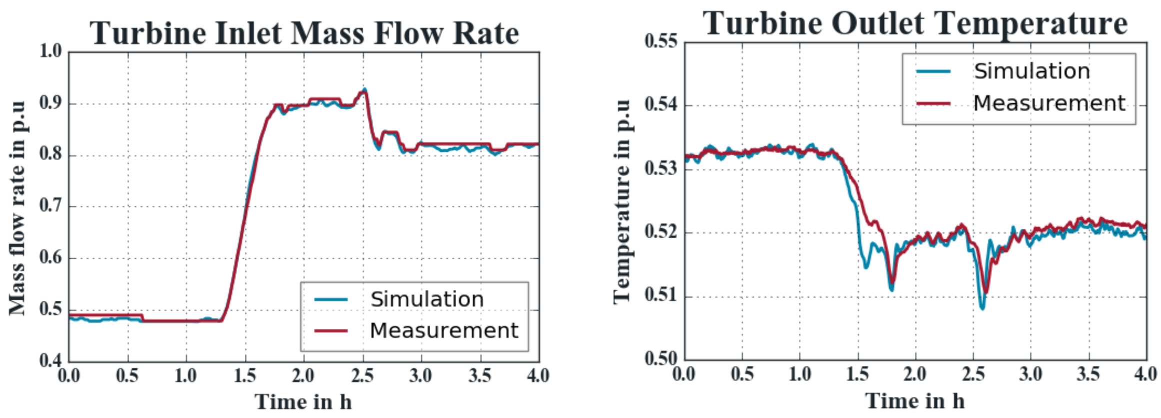

Figure 11: Turbine mass flow rate and outlet temperature validation

The mass flow rate of the validation model fits very well to the measurement over the whole scenario. Especially, the model can represent the load changes very accurately; see e.g. the load change at time 1.5 hours. The measurement of the temperature fits also quite well to the results of the steam turbine model. After the load change and the drops in temperature (1.5 h, 1.75 h and 2.5 h) a delayed reaction of the measured outlet temperature compared to the simulation model can be observed. This results in a maximum error of the temperature of approximately 1 %. The delayed reaction of the temperature can be explained with the lack of thermal masses in the turbine model.

Coal Mill

For validation of the ClaRa+ coal mill model, namely the VerticalMill_L3, the scenario documented in (Niemczyk, Andersen, Bendtsen, & Ravn, 2009) was rebuilt and compared with the model results and the measurement data used for calibration. For validation mill 4 of the Danish power plant at Stignæs was chosen. This mill is one of the widely used Babcock & Wilcox type 10E ball and race mills.

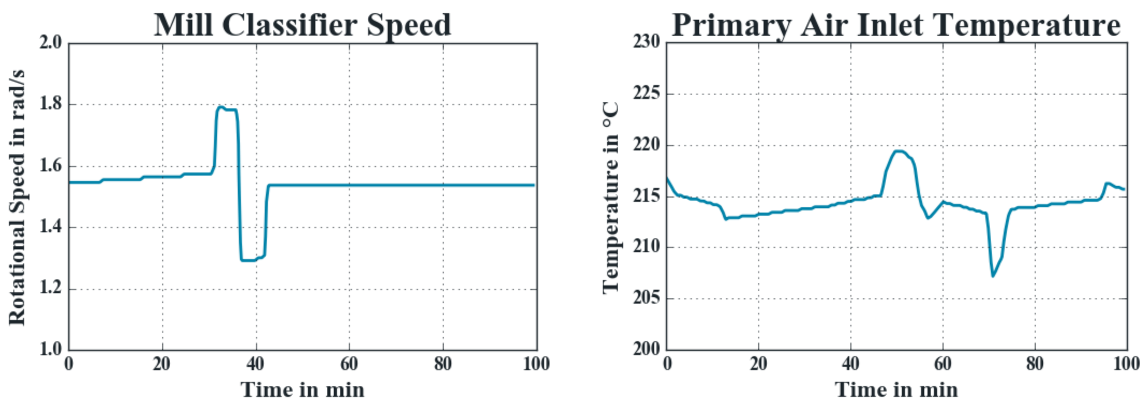

Figure 12: Classifier Speed and Air Inlet Temperature of Mill Validation Scenario

The validation scenario comprehends 100 min of normal operation of the coal mills with the main boundary conditions as can be seen in Figure 12 and Figure 13.

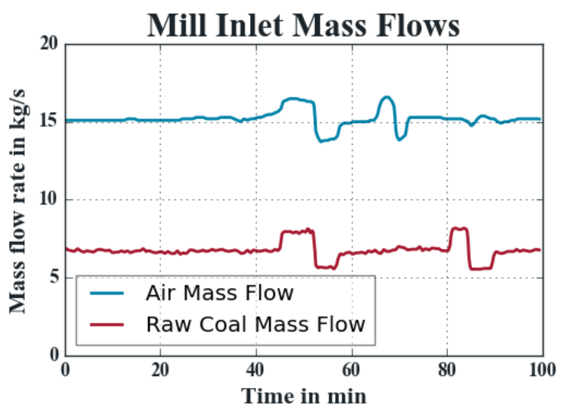

Figure 13: Inlet Mass Flows of Coal Mill Validation Scenario

The raw coal has a moisture content of 6.8 %, the primary air is completely dry and the heat capacity of the coal was set to 1580 J/kg. The last-mentioned value was found to be crucial for the proper calculation of the outlet temperature but was not defined in the original source of the model. The coal's specific heat capacity was therefore adjusted to fit the measurements well.

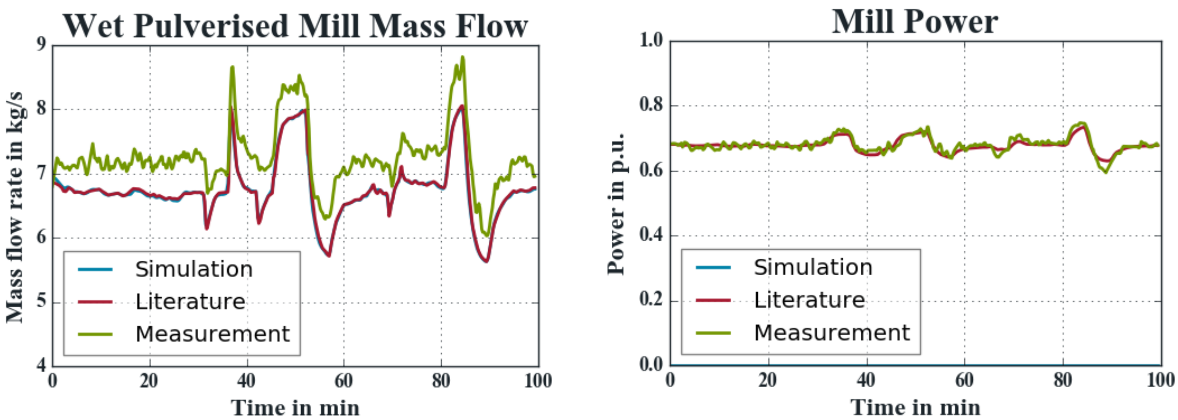

Figure 14: Validation of Coal Outlet Mass Flow and Mill Power

In Figure 14 the mass flow rate of the outgoing coal is shown. The ClaRa$^+$ model agrees perfectly with the model from the literature and the values also comply with the measurement data. Please note that the occurring bias error of the measurement data was also reported in the literature.

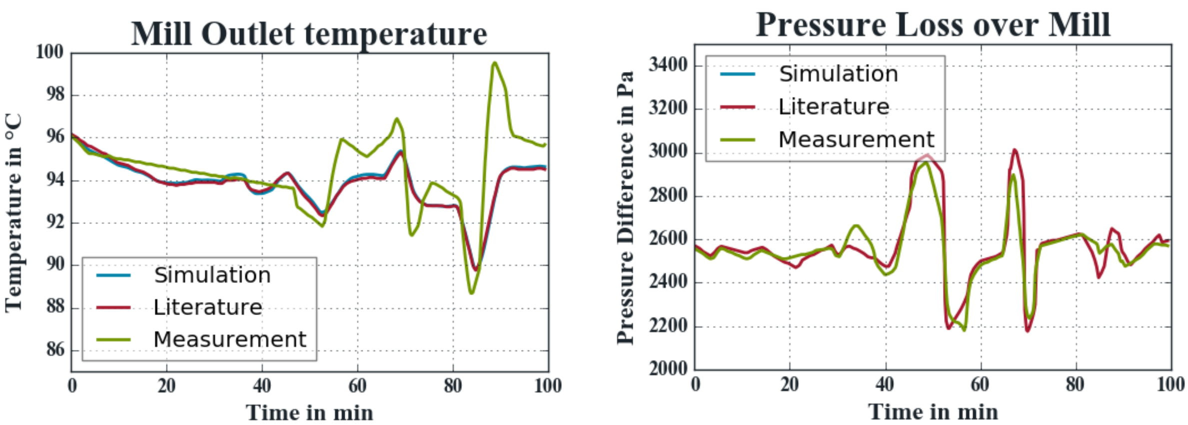

Figure 15: Validation of Mill Outlet Temperature and Pressure Loss

The simulated outlet temperature is similar to the literature's model, see Figure 15. However, the accuracy of the model is limited because only one lumped energy balance is applied for the whole mill. The mill's pressure loss also shows slight deviations from the literature because in the ClaRa$^+$ model no measurement of the primary air differential pressure was assumed and the pressure loss was calculated using a simple quadratic model. This model shows good results compared with the given measurements.

Preheater

The heat exchanger model HEXvle2vle_L3_2ph_CH_ntu is validated using measurement data from a 600 MW hard coal plant. The heat exchanger model features condensation at the shell-side and bases on the concept of Number of Transfer Units (NTU).

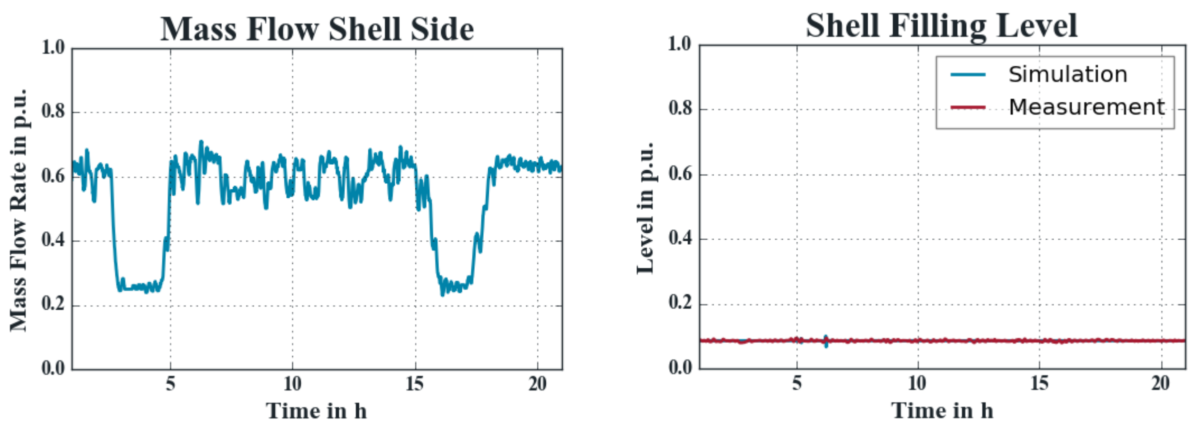

Figure 16: Boundary conditions of preheater validation

The scenario comprises a business as usual operation of a high pressure preheater featuring four large load steps. The boundary conditions for the shell mass flow rate and the level of the heat exchanger are shown in Figure 16. The filling level is controlled by a control valve downstream of the preheater condensate outlet. Furthermore, the mass flow rate at the tube side and the temperatures of the flows going into the preheater are imposed as boundary conditions.

In Figure 17 the comparison of the measurement and the simulation results is plotted. The pressure is slightly under predicted by the model, with a maximum relative error of approximately 4 %. This is an indicator for a slightly overestimated heat transfer of the heat exchanger. An explanation for the effect are the unknown fouling of the heat exchanger at the time of the measurement and the assumption of ideal cross flow in the shell. However, the tube’s outlet temperature is met very well by the model.

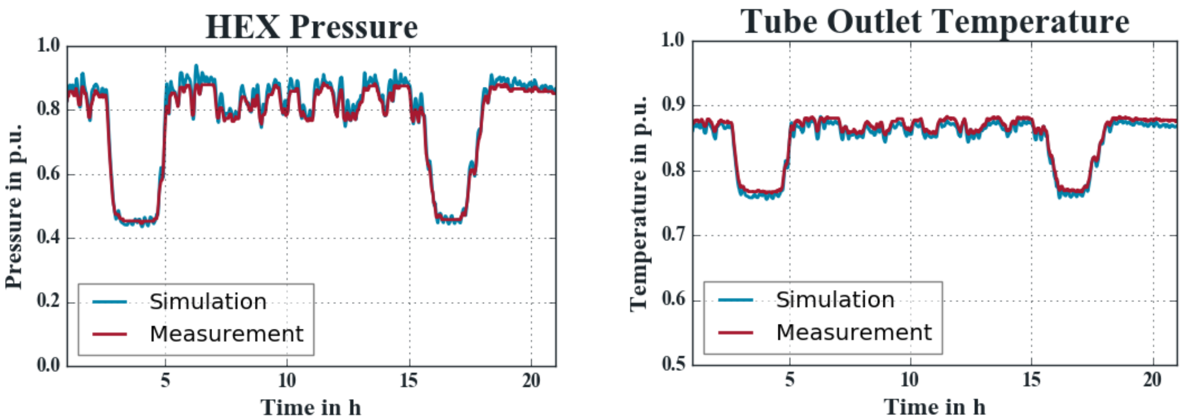

Figure 17: Preheater validation shell pressure and tube outlet temperature

Systems Model Validation

Hard Coal Fired Power Plant in normal Operation

The boiler model of a 600 MW hard coal fired power plant is compared with measurements. It is a once-through boiler with four superheaters and two reheaters. The model of the boiler comprises the flue gas side, the coal handling, the basic control and the water steam side from feedwater pump to turbine inlets including reheating. In consequence, different components of the ClaRa$^+$ from various physical domains have been used to build the overall model. In detail this includes flame room models applying heat transfer and combustion models, the coal mills, models for the evaporator, the superheater and reheaters including spray injection and various control blocks. Thus, the model represents well the broad scope of the library.

Boundary conditions from the measurements are imposed at the economizer inlet, the reheater inlet and the inlet of the coal mills. The scenario is a 20 hours intraday operation with several load changes of the boiler. The boiler starts at full load, goes down to medium load, then to half load and back to full load. Figure 18 shows the flue gas outlet temperature after economiser tube bundle and the reheated steam temperature after the last reheater. Both simulated temperatures are in good accordance with the measurements over the various load points of the scenario.

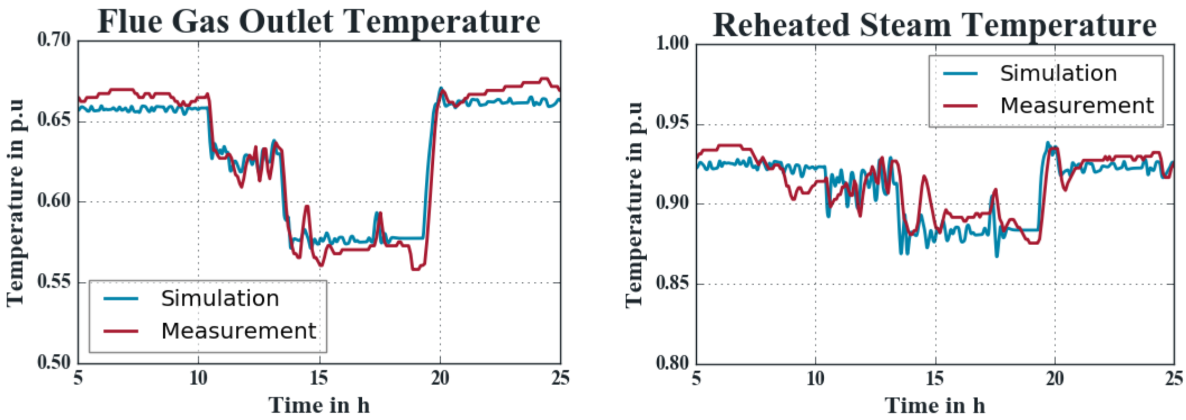

Figure 18: Hard coal boiler flue gas and reheated steam temperature validation

Figure 19 shows the live steam mass flow rate and the live steam temperature. The live steam mass flow rate is the sum of the feedwater mass flow rate and the injection mass flow rates. The result from the simulation fits very well to the measured value. The live steam temperature is controlled by the spray injectors at set point over the whole scenario. This holds true for the simulation and the measurement.

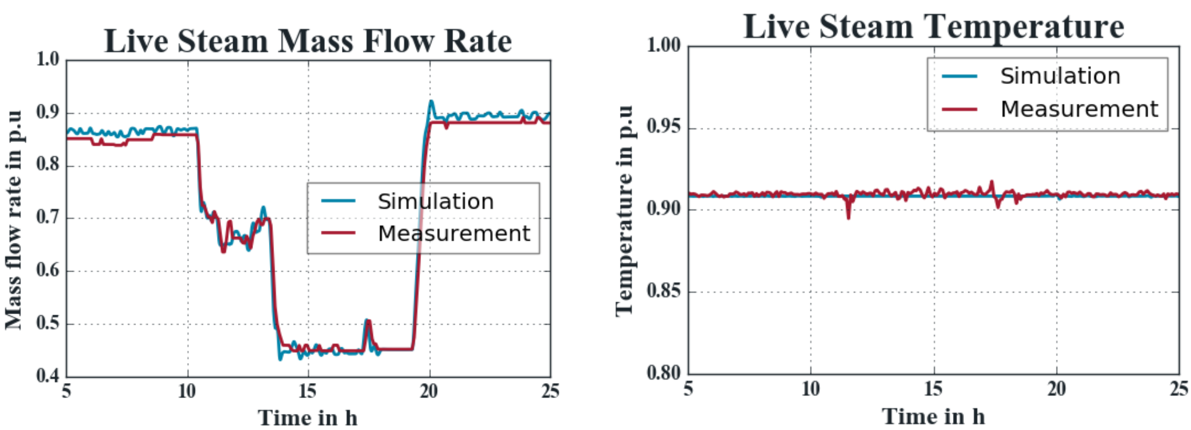

Figure 19: Hard coal boiler live steam mass flow rate and temperature validation

Summary

In this document some examples from the ClaRa+ validation process are presented and discussed in detail. Some of these examples have documentary character while others, e.g. the Super Cannon Experiment, provide valuable information on the scope of the basic thermo-hydraulic physics. The validation model of a complete system, see Hard Coal Fired Power Plant in normal Operation, is built up from models of various physical domains like the flue gas side, the water steam cycle, the control system, etc. Its validation shows the capability of connecting these different domains to meaningful physical models.

The validation of the ClaRa+ is an ongoing process. Each new model requires its own validation, thus the pool of validation models is constantly growing. With extending the scope of the ClaRa+ to new areas of application, for example like supercritical CO_2 cycles, new system validation models become necessary and are added to the pool of validation models. With that procedure, a high quality of the models is guaranteed and their scope can be clearly defined.

Literature Cited

ClaRa+ Development Team. (2018). *ClaRa+ Quality Management: Efforts for Certification According to ISO 9001:2008.*

Diener, R., & Schmidt, J. (December 2004). Sizing of Throttling Device for Gas/Liquid Two-Phase Flow Part 1: Safety Valves. *Process Safety Progress*.

Friedel, L. (1998). *Strömungstechnische Auslegung der Entlastungseinrichtung für druckführende Anlagenteile.*

Fujii, T. (1970). Laminar filmwise condensation of flowing vapour on a horizontal cyclinder.

H. Müller-Steinhagen, K. H. (1986). A Simple Friction Pressure Drop Correlation for Two-Phase Flow in Pipes. *Chem. Eng. Process*.

Henry, R., & Fauske, H. (May 1971). The Two Phase Critical Flow of One-Components Mixtures in Nozzles, Orifices, and Short Tubes. *Journal of Heat Transfer*.

HOLZER, KANZLEITER, T., & STEINHOFF, F. (1977). *SPECIFICATION OF OECD STANDARD PROBLEM NO. 6 - DETERMINATION OF WATER LEVEL AND PHASE SEPARATION EFFECTS DURING THE INITIAL BLOWDOWN PHASE.* Gesellschaft für Reaktorsicherheit.

Idelchik, I. (2006). HANDBOOK OF HYDRAULIC RESISTANCE, 3rd edition.

Mayinger. (1987). Two-Phase Flow Phenomena with Depressurization. *Chem. Eng. Process.*

Müller-Steinhagen, H. (1984). Wärmeübergang und Fouling beim Strömungssieden von Argon und Stickstoff im horizontalen Rohr. *Fortschrittsberichte der VDI Zeitschriften*.

Niemczyk, P., Andersen, P., Bendtsen, J., & Ravn, A. (2009). Derivation and validation of a coal mill model for control. *IFAC Symposium for Power Plant Simulation and Control*.

Riegel, B. (1979). *Experience Super-CANON.* TT/SETRE/79-2-B/BR.

Saha, P., Jo, J., Neymotin, L., Rohatgi, U., & Slovik, G. (1981). *INDEPENDENT ASSESSMENT OF TRAC-PD2 AND RELAP5/M0D1 CODES AT BNL IN FY 1981.*

VDI-Wärmeatlas. (2002). Ga. Wärmeübertragung bei der Strömung durch Rohre.

VDI-Wärmeatlas. (2002). Gh. Wärmeübertragung im Außenraum von Rohrbündelwärmeübertragern mit Umlenkblechen.

VDI-Wärmeatlas. (2002). La. Druckverlust in Leitungen mit Querschnittsänderungen.

Zivi, S. (1964). *Estimation of steady-state steam void fraction by means of the principle of minimum entropy production.*